



Evaluation of Yield Strength Under Small Punch Loading with Different Specimen Thicknesses

Imam Ul Ferdous¹, Nasrul Azuan Alang^{1,*}, Juliawati Alias¹, Norhaida Ab. Razak¹, Zureena Abu Samah²

¹ Structural Performance and Materials Engineering (SUPREME) Focus Group, Faculty of Mechanical and Automotive Engineering Technology, Universiti Malaysia Pahang (UMP), 26600, Pekan, Pahang, Malaysia

² Jabatan Kejuruteraan Mekanikal, Politeknik Sultan Azlan Shah, 35950, Behrang, Perak, Malaysia

ARTICLE INFO

Article history:

Received 24 October 2024

Received in revised form 25 November 2024

Accepted 2 December 2024

Available online 30 December 2024

Keywords:

Finite Element Analysis; Grade 91 steel; small punch test; yield strength

ABSTRACT

Distinguished by its simplicity and cost-effectiveness, Small Punch Test (SPT) enables the evaluation of different types of materials with reliable determination of their mechanical properties. In this study, the yield strength of Grade 91 steel is evaluated under the influence of different thicknesses involving three different yield loads (P_y). A small punch finite element modelling approach was employed to examine the load-displacement (L-D) relationship of the Grade 91 steel. Different empirical relationships were used to determine the dependence of yield strength on specimen thickness. To determine the optimum specimen thickness, the yield load (P_y) and the derived material correlation parameter (α') were considered. Taking these factors into account, the recommended specimen thickness was determined. The predicted yield strength showed that the material correlation coefficient (α) strongly depends on the material and specimen's thickness. The study found a range of $0.31 \leq \alpha \leq 0.48$ for Grade 91 steel. It was also found that the range for the appropriate specimen thickness for SPT is 0.4 mm - 0.75 mm.

1. Introduction

The evaluation of mechanical material properties is crucial for evaluating the structural integrity of plant components in industries such as petrochemical, chemical, and nuclear power plants [1]. However, these materials are subject to degradation over time due to factors such as high temperatures, radiation, and exposure to hydrogen. The careful observation of alterations in mechanical material characteristics is of utmost significance for components in operation. Although there are traditional test methods for assessing the mechanical characteristics of these components, they often have the disadvantages of being expensive and time consuming. Therefore, an alternative approach using the miniature small punch test (SPT) has drawn a lot of interest. The small punch test offers several advantages over traditional test methods, including its cost-effectiveness, shorter test

* Corresponding author.

E-mail address: azuan@umpsa.edu.my

<https://doi.org/10.37934/aram.130.1.1626>

duration, and the use of small samples (8–10 mm in diameter and 0.25–0.5 mm in thickness) [2]. In addition, the test specimens can be obtained directly from the original components, which ensures the authenticity of the results. SPT has been used extensively to predict various properties including, yield strength and UTS [3], Young's modulus [4], temperature transitions from ductile to brittle [5,6], and fracture toughness [7,8]. However, physical testing itself can still be expensive and time-consuming to a certain extent. In such cases, the application of finite element analysis (FEA) for the small punch test proves to be an exceptional alternative to conventional testing methods, particularly when repetitive testing is required. FEA of the SPT provides a comprehensive approach for determining mechanical properties [9]. The Small Punch Test (SPT) FEA shows a force-displacement curve similar to the experimental test, as shown in Figure 1. The curve illustrates the behaviour of ductile materials during small punch testing in terms of deformation. The material's behaviour during loading can be divided into five different zones. Region 1, commonly referred to as linear elasticity, deals with linear-elastic bending deformation, which is determined by the material's Young's modulus and Poisson's ratio. In this region, reversible deformations take place, and a linear relationship between force and deflection is observed. The material enters Region 2, Plastic Bending, as the loading persists, and undergoes a change from elastic to plastic deformation. This is demonstrated by a force-deflection curve that deviates from linearity, signalling the beginning of yielding and permanent deformation. The material's strength coefficient and strain hardening exponent, that control the rate of plastic deformation and work hardening, cause changes in the slope of the curve. The specimen receives further stretching driven on by biaxial load in region 3, Membrane Stretching. The combined effects of biaxial loading and strain hardening result in a steeper L-D curve and more plastic deformation. The material then reaches Region 4, Plastic Instability, which is characterised by thinning, localised plastic deformation, and necking, as the stretching continues. The force-deflection curve experiences oscillations and instabilities as a result of damage initiation caused by void nucleation and coalescence. The break eventually spreads circumferentially in region 5, Fracture Zone, resulting in specimen failure. The L-D curve's load region is identified by an abrupt decline in load, which denotes spectacular fracture and the end of the specimen's load-bearing capacity.

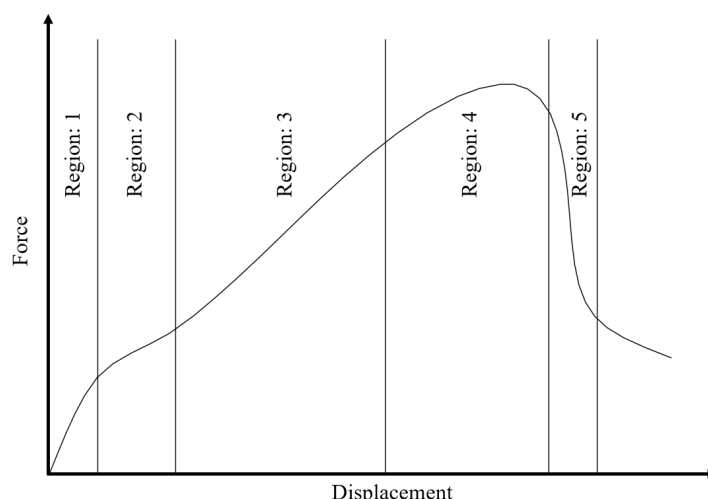


Fig. 1. Force–displacement curve of SPT

There are several factors that influence the outcome of SPT. Among them, specimen shape and thickness, punch ball diameter, clamping force, friction and material play a crucial role [10]. Recognizing the effect of specimen size and shape on the response of SPT is critical to obtaining

accurate and consistent results. Various specimen shapes and sizes have been used at SPT, including round, square, and rectangular specimens. These samples generally have different dimensions. In accordance with the European "Code of Practice" CWA 15627:2006, disk-shaped specimens with a diameter of 8 mm and a thickness of 0.5 mm are recommended for SPT [11]. These specifications provide a standardized approach to testing and ensure comparability of results. In addition, numerical simulations were performed to investigate the response of SPT specimens with different shapes and dimensions. The deformation behavior of SPT is significantly affected by the specimen thickness. The L-D curve, which represents the mechanical response of the material, exhibits remarkable variations as a function of specimen thickness. Understanding these variations is critical for accurate estimation of material properties by SPT. A thin specimen shows a reduction in the pronounced linear elastic component, indicating minimal ability to recover to its original shape after deformation. In addition, thin specimens exhibit lower ductility, i.e., a lower ability to deform plastically without fracturing. On the other hand, relatively thick specimens allow significant plastic indentation and bending, resulting in higher maximum loads and improved ductility. Previous studies [11,12] have emphasized the importance of proposing an optimum range for specimen thickness to obtain consistent and meaningful results in SPT. Small Punch Testing (SPT) uses either a hemispherical ball or a hemispherical punch tip with different diameters to evaluate material properties. While the configuration of the punch does not significantly affect the L-D curve, the diameter of the ball or punch tip does have a notable impact on the retort of the SPT. Previous studies [11,12] have highlighted the effect of the ball diameter on the L-D curve in SPT and emphasized the need to select an appropriate diameter to obtain a reliable and meaningful characterization of the material properties. Furthermore, the scattering effect observed at smaller punch tip diameters [14] underlines the importance of understanding and controlling this parameter during SPT. The clamp force exerted between specimen and die during small punch testing (SPT) is a critical parameter affecting the L-D curve. Proper control of the clamp force is necessary to prevent specimen slippage while avoiding irreversible deformation. Researchers such as Eto *et al.*, [15] and Siegl *et al.*, [16] have used specific clamping forces in their SPT experiments. However, the reasons for choosing these specific clamping force ranges were not provided. A study by Prakash and Arunkumar [17] showed that the prestressing force significantly influences the deformation behavior of the specimen. Raising the clamp force led to elevated peak loads and higher load experienced at smaller displacements. It was shown that the clamping force significantly affected the deformation behavior of the specimen. Increasing the clamping force resulted in higher peak loads and increased loads at smaller displacements. However, further experiments or numerical simulations are required for a more comprehensive understanding of the observed behavior. Small punch tests (SPT) were performed on various classes of materials, including ferritic and austenitic steels, irradiated and nonirradiated materials, and nonferrous alloys. It is evident that the L-D response in SPT varies among these material combinations. However, the typical shape of the L-D curve remains consistent and shows different areas of deformation, as illustrated in Figure 1. Additional parameters such as die fillet radius, chamfer angle, receiving hole diameter, and coefficient of friction between punch and specimen vary across studies. Numerical simulations were used to inspect the influence of these parameters on the L-D curve. However, a comprehensive explanation for the observed response has not yet been discussed in detail. Understanding the relationship between P_y and σ_y , as mediated by the correlation parameter α , is crucial for accurately characterizing the mechanical properties of materials using SPT. The value of α reflects the extent to which P_y can be used to estimate σ_y , and it is influenced by a variety of factors that encompass both intrinsic material characteristics and external testing conditions. Previous studies have revealed that α values for different steels typically fall within the range of 0.36 to 0.41 [17,18]. It is believed that α is affected by material properties,

radiation damage, temperature, and is primarily influenced by test geometry. This study aims to calibrate the material coefficient parameter (α) of Grade 91 steel through small punch finite element analysis in order to determine the yield strength using three different yield loads. Additionally, a recommendation is provided regarding the optimal specimen thickness for future small punch testing.

2. Methodology

2.1 Determination of yield load, P_y

It is imperative to note that the depicted force-deflection curve in Figure 1 serves as an idealized representation. In practical scenarios, the transitions between deformation stages and the identification of critical landmarks, such as the yield load (P_y), may not be as easily discernible. The linear correlation between the tensile yield strength and the load, known as P_y , that distinguishes region 1 and 2 in the SPT test is a widely agreed upon principle among researchers [20]. This correlation is determined by dividing P_y by the square of the initial thickness (t) of the specimen.

However, due to the ambiguous nature of the transition between regions 1 and 2 on the curves, various approaches have been proposed for calculating the P_y load. This study examines three different methods for determining P_y . The first method, referred to as P_{y_I} , is described in the code of practice [11]. P_y is defined as the vertical projection of the point where the two tangents on the test curve intersect. The alternate approach, denoted as P_{y_II} , characterizes the P_y load as the point of intersection between the SPT curve and a straight line parallel to the initial slope of the graph, while incorporating a displacement offset of $t/100$. And the third method refers to as P_{y_III} . Figure 2 illustrates all the methods used to determine P_y .

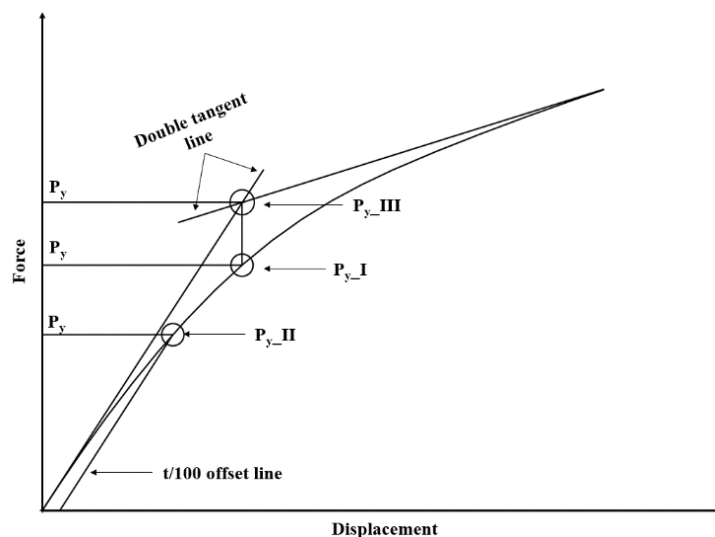


Fig. 2. Determination of P_y

2.2 Determination of Yield Strength (σ_y)

The yield strength of the material is determined by empirically formulating the predicted yield load using the methods previously discussed. There are several empirical relationships that are considered in this study. The constants for these empirical relationships are derived from the yield stress determined in the tensile test. A robust correlation was found among the yield strength projected by SPT and the conventional tensile test. However, it is crucial to acknowledge that the

constant values may differ based on the material and test conditions. For example, Mao and Takahashi [18] used a value of 0.36 as the material correlation parameter for the SUS316 material, while Xu and Zhao [21] used 0.477 for 316 SS. Lee and Kim [22] used 0.23, Finarelli *et al.*, [19] used a range of 0.36-0.41 and Garcia *et al.*, [3] used 0.346 for SA508 C1.3 RPV steel, 316L and Cr steel materials. However, the applicability of these relationships to all materials is subject to debate.

2.3 Determination of correlation parameter α'

For various thicknesses (t), P_y needs to adapt to the changing thicknesses (t) in order to maintain a constant value of P_y/t^2 , as σ_y remains as constant. Consequently, the values of $(\sigma_y \times t^2)$ can be fitted using a linear regression alongside their corresponding P_y values for different thicknesses. The slope derived from this regression, as indicated in Eq. (1) and Eq. (2), represents the parameter α' . This relationship was consistently applied throughout the study. Figure 7 portrays the linear regressions of $\sigma_y \times t^2$ versus P_y for all thicknesses investigated in this research. All methods for calculating P_{y_I} , P_{y_II} , and P_{y_III} were employed for each thickness. As a result, three correlation parameters, α'_1 , α'_2 , and α'_3 were obtained from the slopes of the linear regressions in Figure 7. It is worth noting that the regressions exhibited a good fit, with a minimum regression parameter R^2 of approximately 0.98. In many cases, attempts have been made to determine a representative α by performing linear regressions of σ_y/P_y versus $1/t^2$ for various materials within the same analysis. García *et al.*, [3] conducted an extensive study encompassing several metallic materials with a wide range of strengths. They attempted to establish a 'common' α value as a representative parameter for predicting yield strengths. However, limited agreement was achieved through linear regressions, despite employing various methodologies.

$$\sigma_y = \alpha' P_y / t^2 \quad (1)$$

$$\sigma_y = \frac{\alpha' P_y}{t^2} + C \quad (2)$$

2.4 Finite Element Modelling of the Small Punch Test

Finite element modelling (FEM) was performed using the ABAQUS 6.14 to simulate small punch tests. The FEM simulations are detailed in Figure 3(a), illustrating the components involved. These components include a central axis, a rigid punch indenter with 1.25 mm, upper and lower rigid die, and a deformable disk specimen. To prevent sliding, a friction coefficient of 0.2 was applied. Notably, this study did not incorporate a damage model in the FEM simulations.

Figure 3(b) presents the boundary conditions of the model. The punch's horizontal movement and rotation were restricted to zero, while a 4 mm displacement was applied in the Y direction. Similarly, the axial movement and rotation of both the upper and lower dies were also restrained. In the simulations, twelve different thicknesses of the specimens were considered, ranging from 0.25 mm to 1 mm with a 0.05 mm interval. The disk samples were simulated using axisymmetric linear reduction integral elements (CAX4R). To ensure accurate calculations, a fine mesh optimization technique was employed. The FEM simulations utilized the initial material properties, including the elastic modulus, Poisson's ratio, and true stress-plastic strain, to model the behaviour of the specimens. For this study, Grade 91 steel at room temperature was selected.

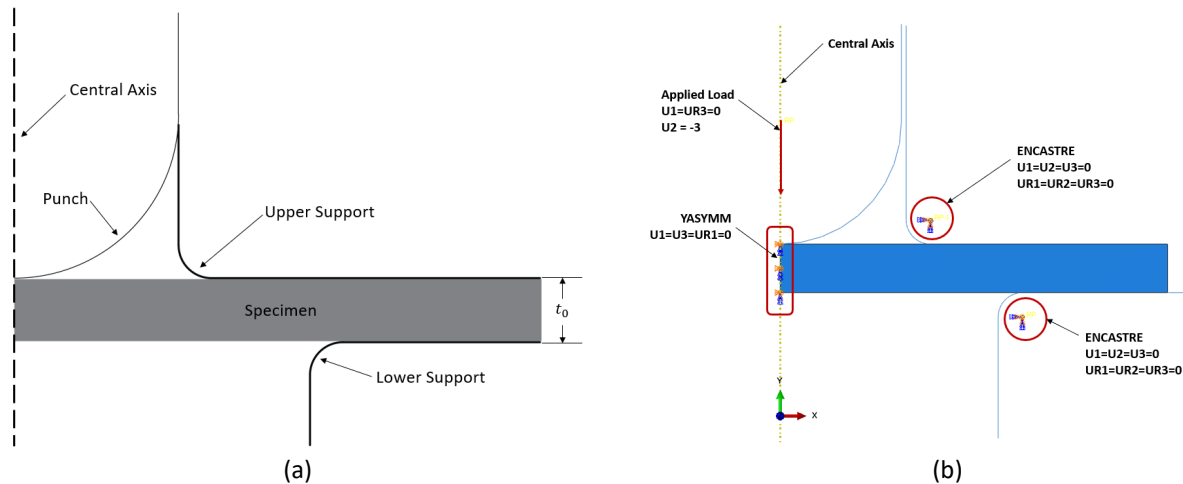


Fig. 3. (a) Different parts of the SPT finite element analysis (b) Boundary condition of the SPT finite element analysis

3. Results and Discussion

Figure 4 compare the experimental results and FE analysis of the L-D relationship of grade 91 steel at different thicknesses (0.4 mm, 0.5 mm, and 0.6 mm) during small punch test at room temperature. The experimental data presented in this figure are taken from the literature [23]. It is noteworthy that the comparison was made on Grade 91 steel with different batches, thus, having different yield strength values (Figure 4). Using different batches of material, the evaluation on the α in predicting the yield strength is made in the next section of the paper. For a thickness of 0.4 mm, the experimentally determined maximum load is 1473 N, while finite element analysis predicts a maximum load of 1282 N. Likewise, the experimental maximum load for a thickness of 0.5 mm is 1926 N, whereas the finite element analysis predicts a load of 1667 N. At a thickness of 0.6 mm, the experimental maximum load is 2393 N and finite element analysis predicts a load of 2106 N. FE predicts a lower P_{max} value because a lower yield strength is applied in the FE analysis. It is worth noting that in the literature [23] a yield strength of 512 MPa is given for the material, while in the FE analysis of this study a yield strength of 358 MPa [24] is used. Table 1 obviously shows that, the yield and maximum loads increased as the yield and ultimate strength increased, respectively. It implicitly illustrates the relationship between the load and the strength.

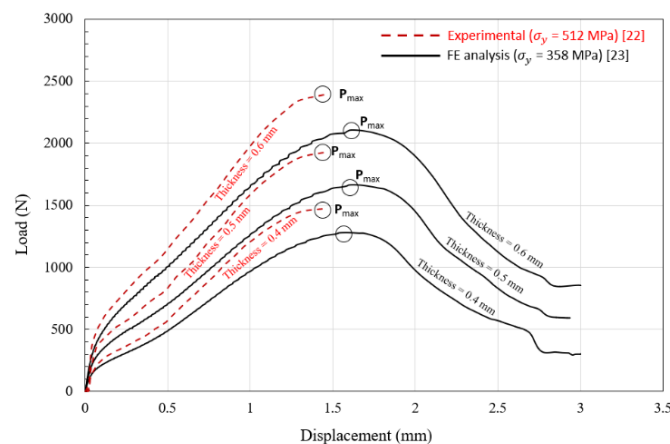


Fig. 4. Comparison between the experimental results and FE analysis of SPT

Table 1

Comparison of yield and maximum loads - experimental and FEA

Thickness	$P_{max}(N)$	$P_{max}(N)$ [23]	P_{y_l}	P_{y_l} [23]
0.4	1282	1473	134	230
0.5	1667	1926	218	390
0.6	2105	2393	342	510

Figure 5 provides valuable insight into the material's response to the punch loads, showing the change in applied load with increasing displacement. Notably, the curve shape shows similarities to the curve shown in Figure 1, indicating different areas of deformation. In addition, the results emphasize that thicker samples require higher loads to achieve the same displacement compared to thinner samples. As the thickness increases, the resistance to the deformation is also increases. For example, the maximum recorded load at a thickness of 0.25 mm is 729.5 N, while at a thickness of 1 mm it reaches 3847 N. This shows how different specimen thicknesses affect the L-D behaviour.

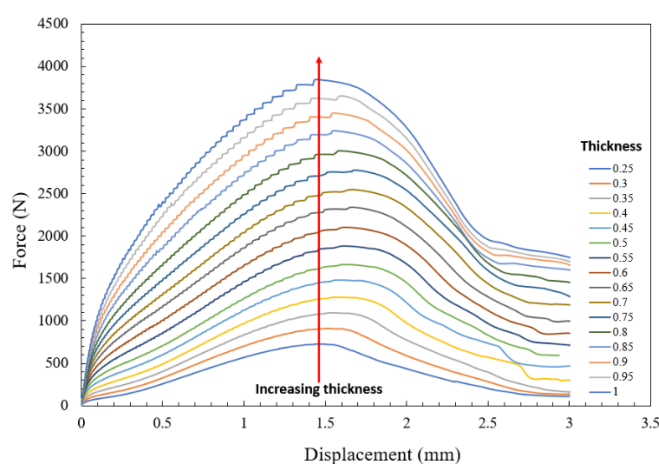


Fig. 5. Force versus displacement obtained using FEA

The relationship between yield strength and specimen thickness is shown in Figure 6. The plot includes empirical relationships with different values of α . In general, it can be observed that as the specimen thickness increases, the yield strength also tends to increase. However, most of the approximations underestimate the actual yield strength, which was 358 MPa. Importantly, the material correlation parameters used in this analysis are specific to different materials, indicating that the α parameter is material dependent. This highlights the need for careful consideration of the correlation parameter in order to accurately predict the yield strength. A notable result of the analysis is the existence of a specific thickness range (0.60 mm to 0.75 mm) in which the yield strength remains relatively constant despite thickness variations. This indicates that within this range the effect of thickness on yield strength becomes negligible. It is worth noting that in the literature [25] it was usually suggested that the a specimen thicknesses of 0.25 mm to 0.5 mm for small punch tests. However, this analysis shows that the correlation parameter plays an important role and must be carefully determined to ensure accurate prediction of yield strength.

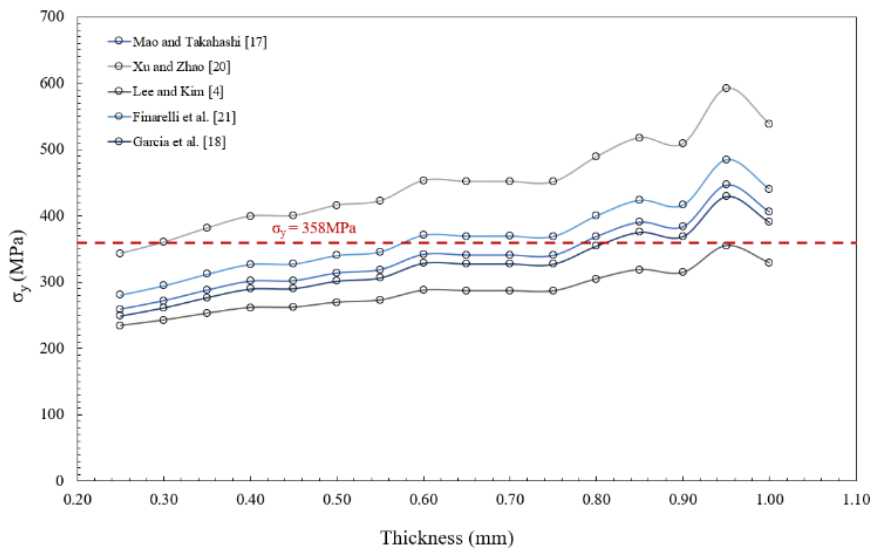


Fig. 6. Yield strength versus thickness obtained using different correlation equations

Figure 7 shows the correlation parameters α'_1 , α'_2 , and α'_3 . It can be observed that α' value is strongly affected by the employed P_y . The variations of α values over the value reported in literature (Figure 6) illustrate the strong dependence on the material. It is also suggested that microstructural parameters (e.g., grain size or strengthening mechanisms) may contribute to the observed segregation into groups [26]. Figure 8 shows a plot of yield strength versus thickness considering different values of α' from Figure 7. The data are consistent with Eq. (2), in which a y-axis intercept is observed. However, Eq. (2) predicts a zero value of yield load, (P_y) when the thickness, t still having finite value. This implies this relationship is somehow invalid particularly when the thickness approaches zero. Further analysis was performed to find a possible solution to this problem.

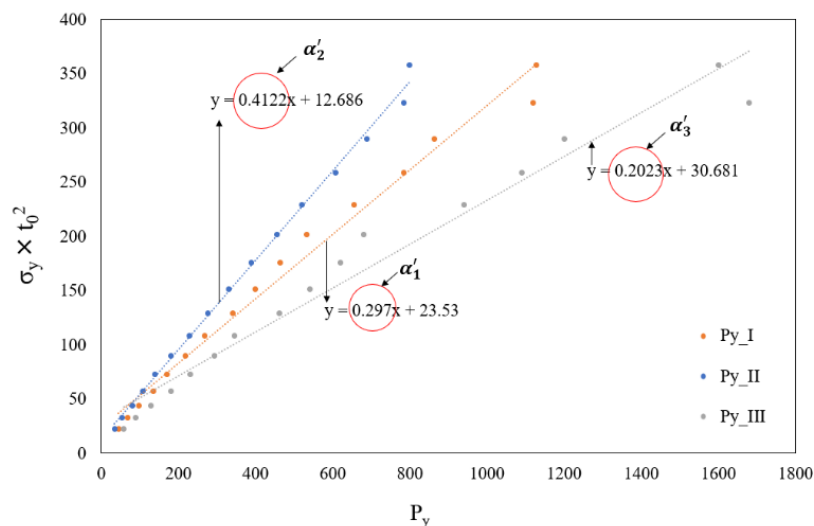


Fig. 7. Determining correlation parameter

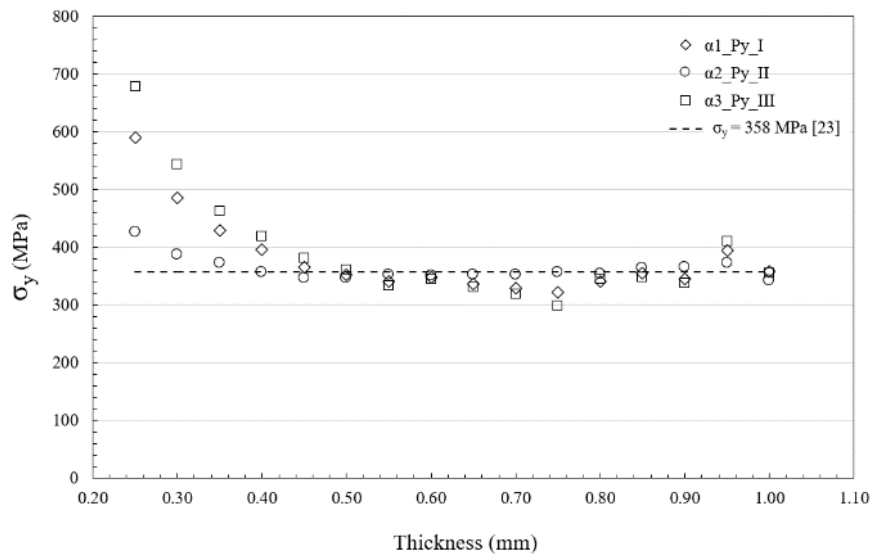


Fig. 8. Yield strength versus thickness obtained using the correlation parameter

The new α'_1 , α'_2 , and α'_3 has been determined using Eq. (1), where y-axis intercept set is zero (Figure 9). It should be noted that the best fitting line is constructed so that it fits most of the data points obtained from FE. Figure 10 presents the plots of newly predicted yield strength versus thickness, where an upper and lower bound of $\pm 10\%$ around the 358 MPa yield strength line has also been added. It is observed that the reliable thickness for SPT is $0.4 < t < 0.75$ mm. Further examination on Figure 10, it becomes evident that Py_I and Py_III provide valid predictions even at lower thicknesses of 0.35 mm. Py_II, on the other hand, demonstrates more stability of the data and remains valid up to a thickness of 0.8 mm. However, it should be noted that Py_III exhibits substantial scatter in the higher thickness region. Considering the recommended code of practice [11], which suggests a specimen thickness of 0.5 mm, and an extension of the code of practice that proposes a thickness range of 0.25-0.5 mm. Present study, however, puts forth a different range of reliable thickness, namely 0.4-0.75 mm. This revised range offers potential for future SPT experiments and provides a more comprehensive understanding of the yield strength variation with respect to thickness.

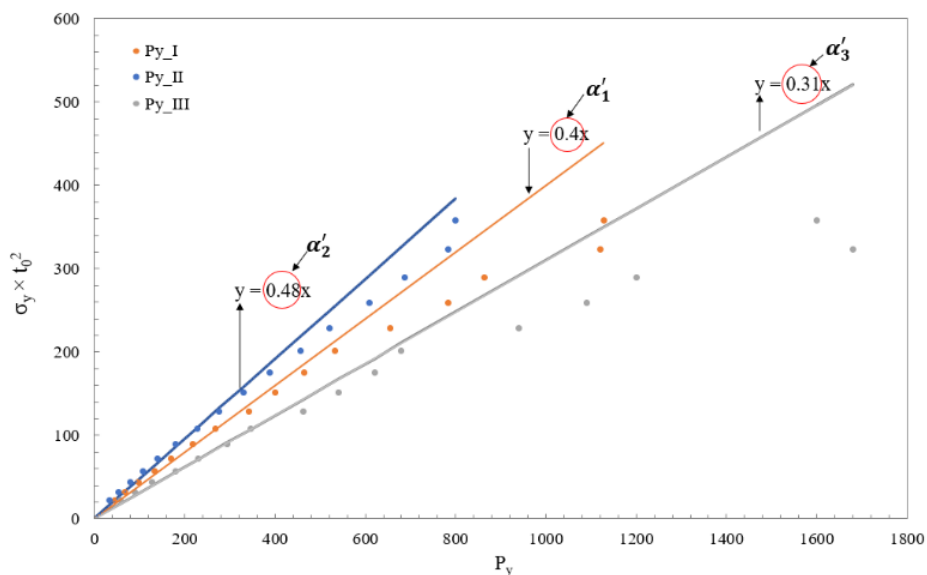


Fig. 9. Determining correlation parameter considering y-axis intercept zero

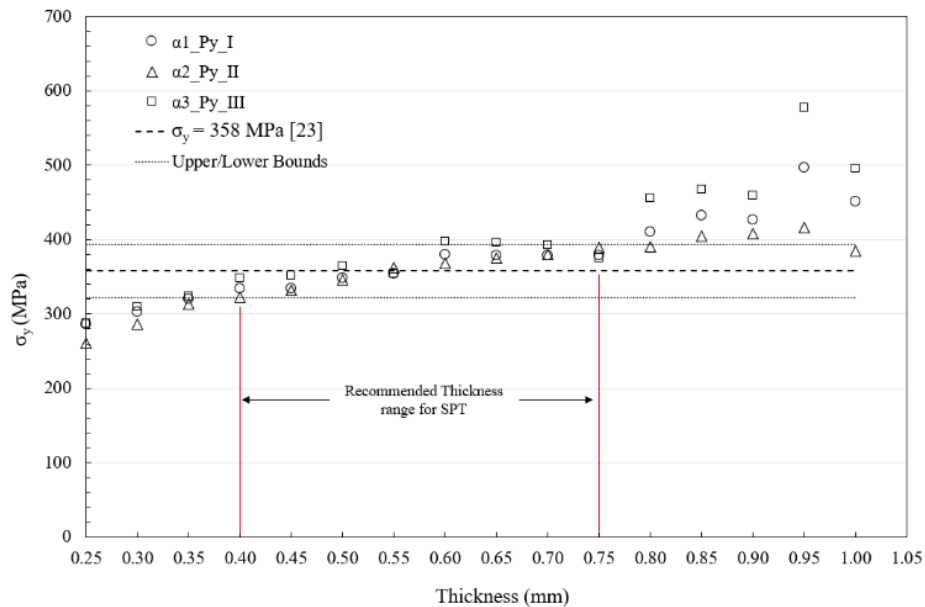


Fig. 10. Yield strength versus thickness obtained using the corrected correlation parameter

4. Conclusions

This study aimed to investigate the reliable thickness of the specimen for small punch test at room temperature using finite element analysis. The results were primarily compared with experimental data from the literature to validate the finite element modelling approach employed in this study. The variations between the experimental and finite element analysis (FEA), in term of yield and maximum loads results can be attributed to differences in the material batches and properties. It was observed that an increase in thickness corresponded to an increase in the applied load, indicating the increased of resistance to deformation. The investigation using different empirical relationships revealed a significant dependence of the material correlation coefficient (α) on the material. The study identified a range of $0.31 \leq \alpha \leq 0.48$ for Grade 91 steel. In addition, the analysis determined a recommended range for specimen thickness for future small punch tests, ranging from 0.4 mm to 0.75 mm.

Acknowledgement

The authors would like to express gratitude to the University Malaysia Pahang for funding this research under the Internal Grant RDU220361.

References

- [1] Zhong, Jiru, Tong Xu, Kaishu Guan, and Jerzy Szpunar. "A procedure for predicting strength properties using small punch test and finite element simulation." *International Journal of Mechanical Sciences* 152 (2019): 228-235. <https://doi.org/10.1016/j.ijmecsci.2019.01.006>
- [2] Ragab, Raheeg, Tao Liu, Ming Li, and Wei Sun. "Membrane stretching based creep damage analytical solutions for thin disc small punch problem." *Journal of the Mechanics and Physics of Solids* 165 (2022): 104928. <https://doi.org/10.1016/j.jmps.2022.104928>
- [3] García, T. E., C. Rodríguez, F. J. Belzunce, and C. Suárez. "Estimation of the mechanical properties of metallic materials by means of the small punch test." *Journal of alloys and compounds* 582 (2014): 708-717. <https://doi.org/10.1016/j.jallcom.2013.08.009>
- [4] Chica, José Calaf, Pedro Miguel Bravo Díez, and Mónica Preciado Calzada. "Improved correlation for elastic modulus prediction of metallic materials in the Small Punch Test." *International Journal of Mechanical Sciences* 134 (2017): 112-122. <https://doi.org/10.1016/j.ijmecsci.2017.10.006>

- [5] Bruchhausen, Matthias, S. Holmström, Igor Simonovski, Timothy Austin, J-M. Lapetite, Stefan Ripplinger, and F. De Haan. "Recent developments in small punch testing: Tensile properties and DBTT." *Theoretical and Applied Fracture Mechanics* 86 (2016): 2-10. <https://doi.org/10.1016/j.tafmec.2016.09.012>
- [6] Guan, Kaishu, Jerzy A. Szpunar, Karel Matocha, and Duwei Wang. "Study on temper embrittlement and hydrogen embrittlement of a hydrogenation reactor by small punch test." *Materials* 10, no. 6 (2017): 671. <https://doi.org/10.3390/ma10060671>
- [7] Kumar, Pradeep, B. K. Dutta, and J. Chattopadhyay. "Numerical development of a new correlation between biaxial fracture strain and material fracture toughness for small punch test." *Journal of Nuclear Materials* 486 (2017): 332-338. <https://doi.org/10.1016/j.jnucmat.2017.01.043>
- [8] Martínez-Pañeda, Emilio, Tomás E. García, and Cristina Rodríguez. "Fracture toughness characterization through notched small punch test specimens." *Materials Science and Engineering: A* 657 (2016): 422-430. <https://doi.org/10.1016/j.msea.2016.01.077>
- [9] Torres, Jonathan, and Ali P. Gordon. "Mechanics of the small punch test: a review and qualification of additive manufacturing materials." *Journal of Materials Science* 56 (2021): 10707-10744. <https://doi.org/10.1007/s10853-021-05929-8>
- [10] Arunkumar, S. "Small punch creep test: an overview." *Metals and Materials International* 27 (2021): 1897-1914. <https://doi.org/10.1007/s12540-020-00783-w>
- [11] CEN (Comité Européen de Normalisation). "Workshop Agreement Small Punch Test Method for Metallic Materials." *Small Punch Test Method Met. Mater.*, Part A and 1–32 Part B, 2006: 1-38.
- [12] Rasche, Stefan, and Meinhard Kuna. "Improved small punch testing and parameter identification of ductile to brittle materials." *International Journal of Pressure Vessels and Piping* 125 (2015): 23-34. <https://doi.org/10.1016/j.ijpvp.2014.09.001>
- [13] Pathak, K. K., K. K. Dwivedi, Manali Shukla, and E. Ramadasan. "Influence of key test parameters on SPT results." (2009).
- [14] Kannan, C., S. Bhattacharya, D. K. Sehgal, and R. K. Pandey. "Effect of specimen thickness and punch diameter in evaluation of small punch test parameters toward characterization of mechanical properties of Cr–Mo steels." *Journal of Testing and Evaluation* 42, no. 6 (2014): 1501-1509. <https://doi.org/10.1520/JTE20130299>
- [15] Eto, Motokuni, Hideaki Takahashi, Toshihei Misawa, Masahide Suzuki, Yutaka Nishiyama, Kiyoshi Fukaya, and Shiro Jitsukawa. "Development of a miniaturized bulge test (small punch test) for post-irradiation mechanical property evaluation." *ASTM special technical publication* 1204 (1993): 241-255. <https://doi.org/10.1520/STP12733S>
- [16] Siegl, Jan, Petr Haušild, Adam Janča, and Radim Kopřiva. "Fractographic aspects of small punch test results." *Procedia materials science* 3 (2014): 912-917. <https://doi.org/10.1016/j.mspro.2014.06.148>
- [17] Prakash, Raghu, and S. Arunkumar. "Evaluation of damage in materials due to fatigue cycling through static and cyclic small punch testing." In *Small Specimen Test Techniques: 6th Volume*. ASTM International, 2015. <https://doi.org/10.1520/STP157620140011>
- [18] Mao, Xinyuan, and Hideaki Takahashi. "Development of a further-miniaturized specimen of 3 mm diameter for tem disk (\varnothing 3 mm) small punch tests." *Journal of Nuclear Materials* 150, no. 1 (1987): 42-52. [https://doi.org/10.1016/0022-3115\(87\)90092-4](https://doi.org/10.1016/0022-3115(87)90092-4)
- [19] Finarelli, D., M. Roedig, and F. Carsughi. "Small punch tests on austenitic and martensitic steels irradiated in a spallation environment with 530 MeV protons." *Journal of nuclear materials* 328, no. 2-3 (2004): 146-150. <https://doi.org/10.1016/j.jnucmat.2004.04.320>
- [20] Arunkumar, S. "Overview of small punch test." *Metals and Materials International* 26 (2020): 719-738. <https://doi.org/10.1007/s12540-019-00454-5>
- [21] Xu, Yuanchao, and Ziqiang Zhao. "A modified miniature disk test for determining material mechanical properties." *Journal of testing and evaluation* 23, no. 4 (1995): 300-306. <https://doi.org/10.1520/JTE10429J>
- [22] J. S. Lee and I. S. Kim. "Evaluation of Mechanical Properties of PRV Clad by Small Punch Tests." *Korean Nucl. Soc.*, 34, no. 6 (2002): 574–585.
- [23] Moreno, M. F. "Effects of thickness specimen on the evaluation of relationship between tensile properties and small punch testing parameters in metallic materials." *Materials & Design* 157 (2018): 512-522. <https://doi.org/10.1016/j.matdes.2018.07.065>
- [24] Ab Razak, Norhaida. "Creep and creep-fatigue interaction in new and serviced exposed P91 steel." *Imperial College London* (2018).
- [25] Matocha, Karel, and Roger Hurst. "Small punch testing-the transition from a code of practice to a European testing standard." *Key Engineering Materials* 734 (2017): 3-22. <https://doi.org/10.4028/www.scientific.net/KEM.734.3>
- [26] Wang, L. Y., Z. J. Zhou, C. P. Li, G. F. Chen, and G. P. Zhang. "Comparative investigation of small punch creep resistance of Inconel 718 fabricated by selective laser melting." *Materials Science and Engineering: A* 745 (2019): 31-38. <https://doi.org/10.1016/j.msea.2018.12.083>